Development of Electrodeless Electric Propulsion Systems Using High-Density Helicon Plasmas: The HEAT Project

Taisei Motomura[1], Shunjiro Shinohara[2], Takao Tanikawa[3], Tohru Hada[4], Ikkoh Funaki[5], Hiroyuki Nishida[6], Konstantin P. Shamrai[7], Takeshi Matsuoka[8], Fumiko Otsuka[9], Timofei S. Rudenko[10], Eiji Ohno[11], Kenji Yokoi[12], and Takahiro Nakamura[13]

[1,11] Department of Advanced Energy Engineering Science, Interdisciplinary Graduate School of Engineering Sciences, Kyushu University, 6-1 Kasuga Koen, Kasuga, Fukuoka 816-8580, Japan,
Tel: +081-(0)92-583-7651, Fax: +081-(0)92-571-8894,
tmoto@aees.kyusyu-u.ac.jp[1], ohno@aees.kyushu-u.ac.jp[11]

[2,6] Division of Advanced Mechanical Systems Engineering, Institute of Engineering, Tokyo University of Agriculture and Technology, 2-24-16 Naka-cho, Koganei, Tokyo 184-8588, Japan,
sshinoha@aees.kyusyu-u.ac.jp[2], hnishida@cc.tuat.ac.jp[6]

[3] Research Institute of Science and Technology, Tokai University,
4-1-1 Kitakaname, Hiratsuka, Kanagawa 259-1292, Japan, tnth@keyaki.cc.u-tokai.ac.jp

[4,9] Department of Earth System Science and Technology, Interdisciplinary Graduate School of Engineering Sciences, Kyushu University, 6-1 Kasuga Koen, Kasuga, Fukuoka 816-8580, Japan,
hada@esst.kyusyu-u.ac.jp[4], otsuka@esst.kyushu-u.ac.jp[9]

[5,8] Institute of Space and Astronautical Science, Japan Aerospace Exploration Agency, 3-1-1 Yoshinodai, Sagamihara, Kanagawa 252-5210, Japan, funaki@isas.jaxa.jp[5], takeshi.matsuoka1@gd.isas.jaxa.jp[8]

[7,10] Institute for Nuclear Research, National Academy of Sciences of Ukraine,
47 Prospect Nauki, Kiev 03680, Ukraine, kshamrai@kinr.kiev.ua[7], rudenkot@kinr.kiev.ua[10]

[12,13] Department of Mechanical Systems Engineering, Institute of Engineering, Tokyo University of Agriculture and Technology, 2-24-16 Naka-cho, Koganei, Tokyo 184-8588, Japan,
50009643303@st.tuat.ac.jp[12], 50010643508@st.tuat.ac.jp[13]

Abstract

In order to develop completely electrodeless next generation plasma thrusters for deep space missions, we have initiated the HEAT (Helicon Electrodeless Advanced Thruster) project. In our scheme, source plasmas are generated by means of the highly efficient helicon-wave discharge; they are then electromagnetically accelerated using external antennas to yield a thrust. The entire process can be achieved without using any eroding electrodes, leading to plasma thrusters of a limitless lifetime.

1. Introduction

The first successful completion of the asteroid sample return mission by the Japanese "Hayabusa" spacecraft could not have been achieved without the μ-10 ion engines, one type of electric thrusters, used for space navigation. However, present-time electric thrusters, ion engines included, suffer a problem of finite lifetime due to the erosion of various electrodes that are in direct contact with dense plasmas. In order to solve this problem, we have initiated the HEAT (Helicon Electrodeless Advanced Thruster) project to develop completely electrodeless advanced-concept electric thrusters. In our scheme, source plasmas are produced extremely efficiently using helicon waves [1,2], or whistler waves propagating in a bounded plasma region, of a radio-frequency (rf) range, ω_{ci} (ion cyclotron frequency) $\ll \omega \ll \omega_{ce}$ (electron cyclotron frequency); they are then electromagnetically accelerated to a high velocity to yield a thrust. The entire process can be achieved without using any eroding electrodes, leading to electric thrusters of a limitless lifetime.

In this paper, some experimental and theoretical approaches to realize completely electrodeless plasma thrusters are presented.

2. Experimental and Theoretical Approaches

Figure 1 shows the configurations of the Rotating Magnetic Field (RMF) [3] and the Rotating Electric Field (REF) [4,5] acceleration schemes. For both schemes, the thrust is generated by the axial Lorentz force which is produced by the azimuthal current and the radial component of the magnetic field ($j_\theta \times B_r$). The RMF and REF vectors ($\tilde{B}_r$ and $\tilde{E}_r$) lie in the cross sectional plane of the plasma and rotate with the drift motion at an RMF frequency of ω' (under the immobile ion assumption) around the z axis. This electron drift is the source of the j_θ[3,4]. In addition to the RMF and REF acceleration schemes, we will also introduce the concepts of the ion cyclotron resonance acceleration and the ponderomotive force acceleration in Sec. 2.5.

Before introducing some details on each scheme, we wish to stress that "nonlinearity" is the key issue in electrodeless plasma acceleration of any sort. This is evident since only time-dependent electromagnetic

978-1-4244-6051-9/11/$26.00 ©2011 IEEE

perturbations (such as rf waves) can penetrate into the plasma to cause its motion, while the net dc thrust should not vanish by time averaging, suggesting that a nonlinear coupling of two ac signals must produce a dc output. According to a conventional wisdom, "nonlinear" means "weak", and thus it is a challenge to generate a large dc power output out of externally applied ac fields (or waves).

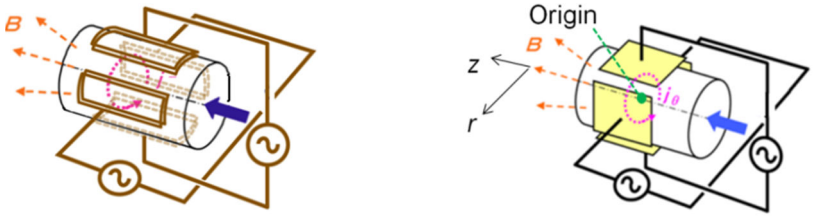

Fig. 1 Configurations of the RMF (left-hand side) and REF (right-hand side) acceleration schemes.

2.1. Experimental Results for RMF

The RMF experiments have been carried out using the Large Mirror Device (LMD) [6] [see Fig. 2(a)]. The RMF coils (10 turns) are mounted on the quartz glass tube (5 cm i.d. and 50 cm length) inserted into the vacuum chamber. To generate a helicon plasma [1,2] to be accelerated by the RMF, a single loop antenna of 4 cm in width is also installed .Each antenna is connected to a separate rf power supply through a matching circuit. The values of the input power and the excitation frequency are ~2 kW and 7 MHz (for the plasma production), and < 1 kW and 1 MHz (for the RMF), respectively. Radially movable standard and directional Langmuir probes at the axial position of z = 15 cm are used to measure the electron density and the ion flow velocity, respectively. In order to measure the RMF penetration, a magnetic probe is placed at the center of the RMF coils. Here, the argon gas pressure is 0.75 mTorr and the electron temperature T_e is typically ~3 eV.

Figure 2(b) shows the initial result of the RMF penetration that is essential to induce the nonlinear j_θ. The ordinate is the magnetic field strength measured by using the magnetic probe at the RMF excitation frequency ω' of 1 MHz, B_{MP}. The abscissa is the RMF coil current, I_{RMF}. In Fig. 2(b), it can be seen that the full penetration of the RMF is achieved at the points of $I_{RMF} \simeq 9$ A and 22 A. This has been confirmed that the B_{MP} in the plasma is in good agreement with the expected curve (dashed line). Here, the dashed line shows the expected calculation field using the coil current in the absence of the plasma. This result is supported by the theoretical results in Refs. 7 and 8. In order to increase the thrust by increasing the induced azimuthal current j_θ, the operating conditions have to be optimized.

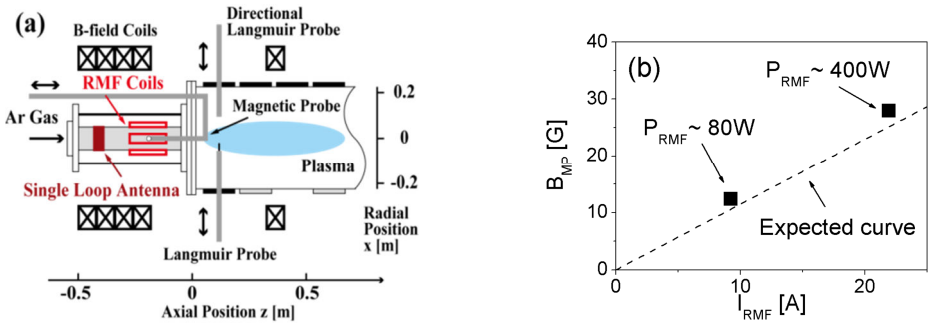

Fig2. (a) Setup of the RMF experiments and (b) initial result of the RMF penetration into the plasma.

2.2. Theoretical approach for RMF

Two important dimensionless parameters to describe the RMF penetration are [9,10], $\lambda = R/\delta$ and $\gamma = \omega_{ce}'/\nu$, where R is the plasma radius, δ is the skin depth, ω_{ce}' is the electron gyro-frequency defined by using the RMF strength, and ν is the summation of the electron-ion and electron-neutral collision frequencies. The former parameter, λ, is a reciprocal of the normalized skin depth, and the latter, γ, states how tightly electrons are attached to the RMF. Under our experimental conditions, the set of values (λ ,γ) falls within a region where the full penetration of the RMF into the plasma ($\gamma/\lambda \gg 1.12$, $\gamma/\lambda > 1.12$:full penetration) is well expected [7,8]. In such a case, the electrons basically make a rigid rotation [7], so that the electron current density is given as $j_\theta(r) = ner\omega'$, where r is the radial distance and n is the plasma density. If the background magnetic field has a radial component, $B_r = B_0 r/2a$, where B_0 is the magnetic field strength on the axis and $a \sim R$ is a constant, then the thrust can be estimated as

$$F = \int_0^R j_\theta B_r 2\pi r dr L = \frac{\pi R}{4a} enL\omega' B_0 R^3, \qquad (1)$$

where L is the axial scale length of the acceleration region. For $\omega' = 6 \times 10^6 sec^{-1}$, $R = 5 \times 10^{-2}$m, $L = 5 \times 10^{-2} m$, $n = 10^{18}$m^{-3}(uniform) and $B_0 = 5 \times 10^{-2}$T, Eq. (1) yields $F \sim 100$mN. We note that the thrust is not reduced significantly even if the RMF penetration is partial since the thrust is mainly produced by the current near the edge of the plasma.

2.3. Experimental results for REF

We have developed a small helicon plasma source for acceleration experiments using the REF scheme at Tokyo University of Agriculture and Technology (TUAT) [4,5] (see the left-hand side of Fig. 3). A glass tube (2.5 cm i.d. and the total length of ~40 cm) is connected to a vacuum chamber. A double saddle type antenna is used for the helicon plasma production [1,2], and the two pairs of flat plate electrodes are used to apply the REF for the plasma acceleration. The excitation frequencies for both the plasma production and acceleration are fixed at 27.12 MHz, and the net-absorbed powers of the plasma production and acceleration are 290 W and 125 W, respectively. The argon gas pressure is fixed at ~0.4 mTorr. The para-perp type Mach probe is used to measure the ion flow velocity, the electron temperature and the plasma density [11] .

The radial profile of the plasma velocity is shown in the right-hand side of Fig. 3. The triangle and cross plots indicate the measurement results before and after applying the REF, respectively. It can be seen that the ion flow velocity is increased in the plasma central region after applying the REF. In addition, both the electron density and temperature are also increased in the plasma central region (not shown). This effect is caused by not only the electromagnetic effect but also the aerodynamic/thermal effect. However, the obtained final flow velocity is not yet enough for the space propulsion application. In order to enhance the plasma acceleration further, the operating conditions have to be optimized with the aid of the theoretical analysis.

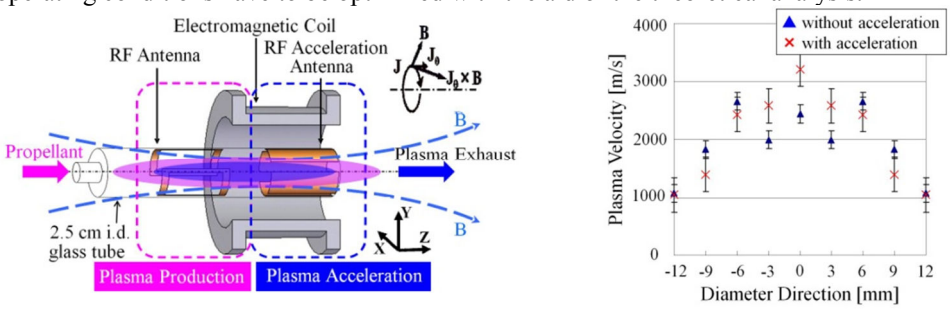

Fig. 3 Experimental configuration of the REF thruster (left-hand side) and the measurement results of the ion flow velocity at 50 mm downstream from the acceleration region (right-hand side).

2.4. Calculation results for REF penetration into dense plasma

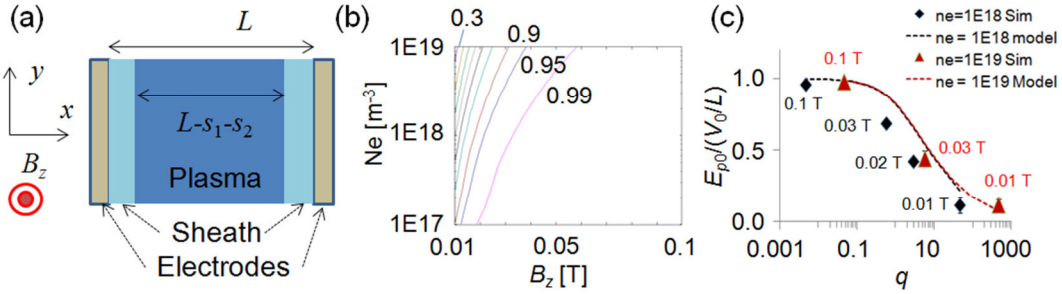

Fig. 6 (a) Configuration of the REF penetration model. (b) Contour plot of penetrated REF calculated by using Eq. (2); V_0 = 100 V, r_0 (uniform r_{ce}) = 0.05 m, f_{rf} = 1MHz. (c) REF strength as a function of q; V_0 = 10 V, L = 0.01 m, and f_{rf} = 100 MHz. The PIC Simulation results are shown for the plasma density of 10^{18} (10^{19}) m^{-3} by diamonds (triangles). The black (red) dotted curve shows REF strength from Eq. (2) for the plasma density of 10^{18} (10^{19}) m^{-3}.

Two circular motions, whose radii are given by $R_D = E_r/\omega B_z$ and the electron gyro radius (r_{ce}) play important roles in the calculation for the REF penetration. The azimuthal current j_θ is found to be proportional to the R_D/r_0 up to an optimum value of $R_D/r_0 \sim 0.4$, then j_θ decreases after the optimum value due to the particle loss to the wall [5]. A 1D analytical model has been developed for the REF field penetration as shown in Fig. 6(a) [12]. The distance between the electrodes is L and the thicknesses of the left- and right-hand side sheathes are $s_1(t)$ and $s_2(t)$, respectively. The REF is driven by applying a time varying potential, $V(t) = \pm V_0 \sin(\omega t)/2$, at each electrode. When the amplitudes of s_1 and s_2 are increased, the plasma current increases linearly. In our analysis, collisional effects are neglected for the sake of simplicity. The solution for the REF, E_{p0}, in the bulk plasma is given by

$$E_{p0}/\frac{V_0}{L} = 1 - \frac{sign(\omega_{ce}-\omega)}{q}\left[\varepsilon - \sqrt{\varepsilon^2 + sign(\omega_{ce}-\omega)q}\right]^2, \qquad (2)$$

with a dimensionless parameter ($q = 8eV_0\omega_{pe}^2/mL^2\omega_{ce}^4$) and the plasma dielectric function ($\varepsilon = 1-\omega^2/\omega_{ce}^2$) in a magnetized plasma. The details of the derivation of Eq. (2) will be reported elsewhere. Here, $sign(\omega_{ce}-\omega)$ is the sign of the $(\omega_{ce}-\omega)$, ω_{pe} is the electron plasma frequency and m is the electron mass. Note that the REF strength is constant due to the charge neutrality of the bulk plasma. The REF strength is plotted in Fig. 6(b) for a set of fixed parameters: r_0, f_{rf} and V_0. The REF strength decreases when the plasma density increases due to the shielding by the

plasma. The REF strength increases when the magnetic field increases due to the reduction of the electron mobility.

In Fig. 6(c), the REF strength from the model is compared with the results from 1D PIC simulations carried out by using the VORPAL code [13]. The ion and electron temperatures are assumed to be 0.3 eV and 5 eV, respectively. The REF strength decreases with the increase in q. The estimated REF penetration from the PIC simulations agrees well with the model prediction.

2.5. Ion Cyclotron Resonance and Ponderomotive Acceleration (ICR and PA)

The ions can be efficiently heated perpendicularly by the ion cyclotron resonance (ICR). In the divergent field, as the ions travel into a region with weaker magnetic field, their perpendicular energy can naturally be converted into the parallel energy, producing the thrust [14]. In addition, by applying the rf waves in such a way that the resonance point coincides with the peak of the wave energy density, the ions can gain parallel acceleration due to the electromagnetic ponderomotive force [15,16]. The ICR and the ponderomotive acceleration (PA) are inseparable, yet the latter is preferred since it is less likely to be influenced by the ion-wall interaction (due to the smaller gyro radius). As an ion crosses the region of the ponderomotive potential, it will gain the kinetic energy [6],

$$\Delta\left(\frac{mv^2}{2}\right) \sim \frac{\pi e^2}{4m\omega^2}\Lambda E_\omega^2 , \tag{3}$$

where E_ω is the rf electric field intensity and $\Lambda = L_B/\rho_z$ is the ratio of the magnetic field gradient scale length to the ion gyro radius defined using the axial ion velocity. Using Eq. (3), the thrust can be estimated as

$$F = \sigma(nmv\pi R^2)v = \frac{\pi^2 R^2 ne^2}{2m\Omega_i^2}\sigma\Lambda E_\omega^2, \tag{4}$$

where σ is a factor representing the effect of the ion-neutral collisions. Substitution of $E_\omega = 10^3 V/m$, $\sigma = 0.1$ and $\Lambda = 1$ yields $F \sim 50\text{mN}$. Here the total penetration of the electric field into the plasma is assumed. This of course is a highly optimistic simplification, and the plasma shielding effect must be included for making more realistic estimates.

3. Conclusions

In order to develop next generation advanced plasma thrusters for deep space missions, the HEAT (Helicon Electrodeless Advanced Thruster) project has been initiated. The project includes experimental and theoretical studies of various aspects of electrodeless plasma thruster concepts.

The RMF penetration into the plasma and the plasma acceleration effects by the REF are experimentally confirmed. The conditions for the REF penetration are also derived from the PIC simulations as well as from a simple model analysis. In addition, the theoretical analysis is under way for the acceleration scheme that uses the ponderomotive force effects. The project has to be optimized using various experimental and theoretical approaches in order to solve challenging problems for the successful development of a completely electrodeless plasma thruster system.

4. Acknowledgements

The authors would like to acknowledge the great contributions made by late Prof. Kyoichiro Toki. This work has been supported by the JSPS Grant-in-Aid for scientific research (S: 21226019). One of the authors (T.M.) is the Research Fellow of the JSPS.

5. References

1. 1.R.W. Boswell, Phys. Lett. **33A**, 1970, pp. 457.
2. S. Shinohara, Jpn. J. Appl. Phys. **36**, 1997, pp. 4695.
3. I. R. Jones, Phys. Plasmas **6** , 1999, pp. 1950.
4. K. Toki, S. Shinohara, T. Tanikawa, and K. P. Shamrai, Thin Solid Films, **506-507**, 2005, pp. 597-600.
5. H. Nishida, S. Shinohara. T. Tanikawa. T. Hada, I. Funaki, and T. Matsuoka, *et al.*, AIAA2010-7013, 46th AIAA/ASME/SAE/ASEE Joint Propulsion Conference & Exhibit, Nashville, TN, USA, 25 - 28 July, 2010.
6. S. Shinohara, S. Takechi, and Y. Kawai, Jpn. J. Appl. Phys. **35**, 1996, pp. 4503.
7. R. D. Milroy, Phys. Plasmas **6**, 1999, pp. 2771.
8. M. Inomoto, IEEJ Trans. FM. **128**, 2008, pp. 319.
9. W. N. Hugrass, Aust. J. Phys. **38**, 1985, pp. 157.
10. A. L. Hoffman, H. Y. Guo, K. E. Miller, and R. D. Milroy, Phys. Plasmas **13**, 2006, pp. 012507.
11. A. Ando, T. Watanabe, T. Watanabe, H. Tobari, K. Hattori, and M. Inutake, J. Plasma Fusion Res. Ser. **81**, 2005, pp. 6.
12. Private communications, K. P. Shamrai, and T.S. Rudenko (2010).
13. http://www.txcorp.com/products/VORPAL/
14. E. A. Bering III, F. R. Chang Díaz, J. P. Squire, T. W. Glover, M. D. Carter, and G. E. McCaskill, *et al.*, Phys. Plasmas, **17**, 2010, pp. 043509, and references therein.
15. I. Y. Dodin, N. J. Fisch, and J. M. Rax, Phys. Plasmas **11**, 2004, pp. 5046.
16. G. Emsellem, The 29th International Electric Propulsion Conference, Princeton Univ., 31 Oct. - 4 Nov., 2005, IEPC-2005-156.